2023

Measurement of Ankle Joint Kinematics Using Imus during Countermovement Jumps and Lateral Skater Jumps

Ifeoluwa Olawore

Illinois State University, victorifeoluwa@gmail.com

Follow this and additional works at: https://ir.library.illinoisstate.edu/etd

MEASUREMENT OF ANKLE JOINT KINEMATICS USING IMUs DURING COUNTERMOVEMENT JUMPS AND LATERAL SKATER JUMPS

IFEOLUWA OLAWORE

22 Pages

This study compared Inertial Measurement Unit (IMU) and Optical Motion Capture (OMC) systems in measuring peak ankle angles and Range of Motion (ROM) during Countermovement Jumps (CMJ) and Lateral Skater Jumps (LSJ). Ankle angles in pitch, roll, and yaw were determined by integrating gyroscope data, aligning with foot flat reference, and fusing with accelerometer-derived inclination angles using a complementary filter. We hypothesized that IMU-based methods would parallel OMC in capturing peak angles and ROM during CMJ and LSJ landings, with accuracy and reliability assessed via Root Mean Square (RMSE) and Intraclass Correlation (ICC) statistics. For CMJ, high accuracy and reliability were observed in the Peak Positive Frontal angle with RMSE of 6.72° and ICC of 0.517. However, LSJ displayed lower performance, with no metric reaching an ICC > 0.5 or an RMSE < 10°. The study suggests limitations of IMU in accurately capturing ankle joint kinematics in dynamic jumps using these methods.

KEYWORDS: Sensors, Kinematics, Dynamic, Algorithm, Filter, Integrate

MEASUREMENT OF ANKLE JOINT KINEMATICS USING IMUs DURING COUNTERMOVEMENT

JUMPS AND LATERAL SKATER JUMPS

IFEOLUWA OLAWORE

A Thesis Submitted in Partial
Fulfillment of the Requirements
for the Degree of

MASTER OF SCIENCE

School of Kinesiology and Recreation

ILLINOIS STATE UNIVVERSITY

2023

MEASUREMENT OF ANKLE JOINT KINEMATICS USING IMUs DURING COUNTERMOVEMENT

JUMPS AND LATERAL SKATER JUMPS

IFEOLUWA OLAWORE

COMMITTEE MEMBERS:

Michael Torry, Chair

Daniel Feeney

Tyler Kybartas

ACKNOWLEDGMENTS

CONTENTS

TABLES

CHAPTER I: INTRODUCTION

The methodology employed in three-dimensional (3D) human motion analysis determines the limitations in assessing human movement for athletic performance, injury prevention and rehabilitation progress [1–3]. Optical Motion Capture (OMC) has historically been the gold standard, renowned for its accuracy and reliability in tracking even the most complex of motions[4,5]. However, spatial restrictions, significant financial and expertise demands, susceptibility to marker occlusion, and the substantial subject preparation and equipment setup time often limit its applicability, especially in real-time field settings. Inertial Measurement Unit (IMU) sensors have emerged as an alternative due to their adaptability, portability, and user-centric nature [6,7]. Numerous algorithms have been developed to create accurate angular kinematic data from single or multiple body segments using IMUs inside and outside the laboratory setting [6,8–15]. For example, Seel et al[13] developed a novel algorithm using complimentary filter to calculate flexion/extension joint angles between a prosthetic and a contralateral leg during ambulatory movements and achieved deviations less than 0.6° and more than 3.0° respectively between IMU and OMC based methods. Similarly, Song et al[14] tested seven different algorithms in a model-based simple experiment and discovered that all methods showed high accuracy (RMSE<6) for roll and pitch angles and five of them stayed accurate in yaw angle calculations. These algorithms which sometimes omit magnetometer data to avoid drift introduced by magnetic interference [8,10,12–20], aim to emulate the accuracy and reliability of OMC results, particularly in capturing relative joint angles and spatiotemporal metrics. To further validate its efficacy, it is imperative to test these known algorithms during more dynamic motions.

Dynamic movements like Countermovement Jump (CMJ) and Lateral Skater Jumps (LSJ) serve as benchmarks to evaluate athletes' reactive strength, power production capabilities, and readiness for return to activity via metrics including peak joint angles and joint Range of Motion (ROM)[21–23]. Ankle mechanics during these jumps, which contribute to approximately 22–23% of the take-off velocity, are especially significant[24]. As Panoutsakopoulos and Bassa[21] observed, female adolescent volleyball players with greater ankle flexibility exhibit superior vertical jump performance, underscoring the importance of ankle mechanics in jump-centric sports like volleyball. Additionally, specific ankle angles, such as increased peak inversion and internal rotation, have been linked to injury risks[25].

Streamlined and computationally efficient IMU-based motion analysis methods offer significant advantages over OMC, including wide-ranging clinical applications and the ability to conduct meaningful out-of-lab studies. This study aimed to: (a) evaluate the accuracy and reliability of simple algorithms for detecting jump events and computing ankle angles using IMUs in both CMJ and LSJ; and (b) compare the peak ankle joint angles and Range of Motion (ROM) derived from both IMUs and Optical Motion Capture (OMC) systems in all three axes (pitch, roll, and yaw) during the landing phases of these jumps. It was hypothesized that the IMU algorithms would match the accuracy and reliability of OMC in determining peak ankle joint angles and Range of Motion (ROM) during the landing phases of CMJ and LSJ, as evaluated by Root Mean Square Error (RMSE) and Intraclass Correlation (ICC) measures. Accuracy assessed the deviation of the IMU from the OMC measurements while reliability determined the consistency of IMU readings over repeated trials.

CHAPTER II: METHODOLOGY

This cross-sectional observational study utilized deidentified data provided by the Performance Fit Lab (PFL) of Boa® Technologies. The study involved the testing of 10 subjects. Participants were instructed to perform 8 repetitions of CMJ followed by 8 repetitions of LSJ at their own pace. The CMJ required participants to initiate from a standing position with each leg positioned on a separate force platform (Bertec, Columbus, OH). Hereafter, they performed a downward motion by flexing the knees and hips, then immediately spring upwards into a jump, arms extended overhead, and legs fully straightened during flight. They subsequently landed back onto the same starting plates. The LSJ then had participants leaping sideways from one foot to the other, over a length one-third of their height, mimicking the movement of a speed skater. The right foot targeted and landed on a force plate while the left foot landed on flat ground.

The study utilized Blue Trident IMUs (iMeasureU, Vicon Ltd., London, UK) which comprise a triaxial accelerometer capable of measuring up to ±16 g with two sampling rates of 1125 Hz (high-g) and 1160 Hz (low-g), a magnetometer with a range of ±4900 µT operating at 112.5 Hz, and a gyroscope with a maximum detectable rotation rate of ±2000°/s and a sampling rate of 1125 Hz. The magnetometer data was excluded from the analysis, owing to concerns regarding potential magnetic interference and associated data drift[18]. One IMU was securely positioned on the distal third of the right tibia, just above the ankle, while the other was placed on the arch of the foot, directly over the navicular and cuneiform bones. The foot and shank IMUs were oriented such that its y-axis was aligned with the sagittal plane, the z-axis with the transverse plane, and the x-axis with the frontal plane. Before collecting data, to maximize

accuracy, the IMUs were calibrated by waving them in a figure-of-eight for at least 10 seconds and rotating them on a flat surface, as directed in the Vicon IMU documentation[26].

OMC setup involved 12 overground infrared cameras (Nexus v.2.12, Vicon Motion Systems Ltd., Oxford, UK)) operating at a frequency of 200 Hz. Using a 6 Degrees of Freedom (DOF) lower limb model, marker clusters consisting of three markers each were placed on the foot (on the heel/calcaneus), and on the shank, approximately midway along the tibia. The OMC system leveraged this 6 DOF model built on The MotionMonitor xGen software (Innovative Sports Training Inc, IL, USA) to generate ankle joint kinematics along three rotational axes – flexion/extension, internal/external rotation, and inversion/eversion. Post-processing involved the application of a 4th order Butterworth filter (10Hz cutoff) to smooth the marker trajectories. The ankle joint was modelled to reflect its full multi-axial movement capabilities and primarily designated by the tips of the lateral and medial malleoli to establish the axis of rotation. This approach allowed for measurement of the three rotations, capturing the complex kinematics of the joint. Toe off and landing events in the OMC were determined using data from the force platforms by a vertical ground reaction force-based threshold.

IMU computations began with a preprocessing approach[15,17] involving merging data from high-g (1,600Hz) and low-g (1,125Hz) accelerometers to prevent saturation during dynamic movements. Python programming language (Python Software Foundation, version 3.12.0) was utilized for all IMU-based data manipulations. When the low-g accelerometer neared saturation threshold ±16 g, it switched to high-g readings. Subsequently, data from foot and shank IMUs were aligned using cross-correlation, ensuring synchronized motion data. Jump phases in the IMU data were identified using vertical acceleration guided by methodologies validated by

Schmidt et al, Jaitner et al as well as Smith and Bedford[23,27,28]. In brief, the algorithm starts by reading vertical acceleration data from the IMU's accelerometer readings. From time T = 0, when acceleration surpasses an empirically defined take-off threshold and trends towards a free-fall value (-9.81m/s^2), the peak indicates the take-off phase. The subsequent acceleration peak signifies the landing phase, with its detection based on achieving a separate empirically defined threshold based on the minimum peak values observed graphically. For a jump to be classified as valid: (a) Both take-off and landing accelerations must exceed their respective thresholds, and (b) The time duration between these peaks, dt, should fall within an empirically defined time window between 0.6s-1s. After identifying the landing phase index, the algorithm defines a window leading to take-off to identify the foot's flat position by examining the acceleration rate of change. A consistent near-zero derivative indicates the foot's flat position focusing on when the acceleration data exhibits relatively static or low activity.

To ensure anatomical meaningfulness of the calculated ankle angle and consistency across subjects, the local sensor coordinate system was aligned to the reference laboratory system. Given the three-dimensional nature of human movement, the Euler angles of pitch, roll, and yaw served as the primary means to represent the orientation of body segments in space. The pitch represented rotation about the anteroposterior axis, encapsulating the movements of plantarflexion and dorsiflexion; Roll captured rotation about the mediolateral axis, indicative of foot inversion and eversion while yaw denoted rotation about the vertical axis representing, internal and external rotation. The sequence of these rotations was maintained in line with the recommendations of the International Society of Biomechanics (ISB) as detailed by Wu et al[29]. During alignment, the acceleration vector was normalized, and its rotation axis was determined

5

using the cross product with the lab's gravitational vector, producing vector "C". The required

rotation magnitude was calculated, resulting in value "D", from which a rotation matrix, "R", was

formed. Euler angles were then extracted from R to set as initial orientations to align the IMU

data for anatomically accurate orientations.

Before integrating the angular velocities from the gyroscope to yield the orientations of

the foot and shank, the data was filtered.   Specifically, gyroscope data and accelerometer data

were low-pass filtered (Hz) to eliminate high-frequency disturbances[6,13,14]. The cut-off for the

filtering was determined through a Fast Fourier Transform (FFT) of each dataset. The integration

methodically aggregates the angular alterations over consecutive time frames producing the

cumulative angular shift for each axis through the landing phase. This is represented in equation

1.

$$\Theta(t) = \int Filtered\ Gyro\ Data(t)dt \qquad\qquad (1)$$

Where $\Theta(t)$ represents the angular orientation at time t, and dt is the sample time interval. To

counteract the drifts caused by integration errors, orientation angles from the foot-flat phase

were utilized for linear dedrifting[15,17]. By aligning the angles from gyroscopic integration with

this initial foot-flat reference, a more accurate representation of the movement dynamics was

achieved. To further remove drifts from the obtained orientations in roll and pitch angles,

acceleration inclination angles were calculated and incorporated for use[6,14]. For the pitch and

roll inclinations, the respective orientations θ_{pitch} and θ_{roll} were calculated using the equations 2

and 3 below:

$$\theta_{pitch}(t) = -\arctan\left(\frac{a_y(t)}{\sqrt{a_x(t)^2+a_z(t)^2}}\right) \qquad\qquad (2)$$

$$\theta_{\text{roll}}(t) = -\arctan\left(\frac{a_x(t)}{\sqrt{a_y(t)^2 + a_z(t)^2}}\right) \tag{3}$$

A complementary filter was then employed to synthesize accelerometer and gyroscope data, enhancing sensor fusion by leveraging the strengths of both sensors. This method combines the high-frequency sensitivity of the gyroscope with the low-frequency stability of the accelerometer. The accelerometer is known to be sensitive to both gravitational and linear accelerations of the body segment. By harnessing both strengths, the fusion applies to provide a combined gain equal to one—effectively blending the data sets with appropriate weights.

The weighting factor/filter coefficient, γ, calculated in equations (4) from τ in equation (5), computationally favored gyroscope angles, to utilize over 99% of the sensor fusion, reflecting its high dynamic accuracy. The remaining percentage was contributed from the accelerometer-based angles, providing low-frequency orientation cues.

$$\gamma = 1 - \frac{\tau}{\tau + dt} \tag{4}$$

$$\tau = \frac{\omega drift}{e_{tol}} \tag{5}$$

Where dt was the average difference in time interval, τ was the time constant, ω_{drift} was the gyroscope's drift rate and e_{tol} is the tolerance threshold[13,14]. The measured ω_{drift} was 0.30°/s while the e_{tol} was set to 3° which is half the acceptable error tolerance threshold[13]. Thus, τ was 0.1Hz which sets the frequency threshold for blending the accelerometer and gyroscope data orientations, influencing γ. The complementary filter was computed using the equation below:

$$\vartheta_{cf}(t) = (1 - \gamma) \times (\vartheta_{gyro}(t) + \int Gyro\ Data(t)dt) + \gamma \times \theta_{accel}(t) \tag{6}$$

For each axis – roll, pitch, and yaw – the angular difference between shank and foot orientations computed represents the ankle angle[13,14].

From this data, peak angles, and the ROM of both IMU and OMC obtained angles in both CMJ and LSJ were derived. The considered periods for both systems were the landing period (between foot contact and the subsequent takeoff). Root Mean Square Error (RMSE)[30,31] was used to compare both systems using Equation (7) below:

$$\text{RMSE} = \sqrt{\frac{\sum_{i=1}^{N}(Y(i)-\hat{Y}(i))2}{N}} \qquad (7)$$

Where:

- $Y(i)$ represents the observed value from the OMC system at the ith instance.

- $\hat{Y}(i)$ is the calculated value from the IMU at the ith instance.

- N is the total number of observations.

RMSE values less than 10 indicated high accuracy. Intraclass Correlation was used to assess reliability of IMU angle measurements[20]. ICC values lie between 0 and 1, with values close to 1 indicating high reliability and values near 0 indicating low reliability[32]. All statistical analysis was done using Python Programming language.

CHAPTER III: RESULTS

Table 1 summarizes the ICC and RMSE values for both CMJ and LSJ across all metrics below while Appendices B, C and D show the jump detection graph results and the graphical comparison of two jumps of two subjects.

Metric	CMJ		LSJ	
	ICC (95% CI)	RMSE (°)	ICC (95% CI)	RMSE (°)
ROM Frontal	0.273 (-0.180, 0.720)	11.27	0.045 (-0.100, 0.380)	58.37
ROM Sagittal	0.114 (-0.370, 0.640)	31.01	0.027 (-0.120, 0.370)	55.48
ROM Transverse	-0.110 (-0.300, 0.330)	16.41	0.020 (-0.050, 0.220)	79.7
Peak Positive Frontal	0.517 (-0.040, 0.850)	6.72	0.217 (-0.300, 0.700)	31.71
Peak Positive Sagittal	-0.054 (-0.320, 0.420)	34.33	0.057 (-0.130, 0.430)	36.78
Peak Positive Transverse	-0.068 (-0.360, 0.430)	15.16	-0.055 (-0.280, 0.380)	33.65
Peak Negative Frontal	0.036 (-0.190, 0.450)	13.47	-0.002 (-0.050, 0.150)	37.86
Peak Negative Sagittal	0.167 (-0.240, 0.640)	19.92	0.059 (-0.430, 0.600)	35.45
Peak Negative Transverse	-0.457 (-0.940, 0.270)	15.91	-0.136 (-0.280, 0.310)	64.42

1 : Comparison of ICC and RMSE Values for Ankle Joint Angles in CMJ and LSJ.

The reliability of IMU measurements compared to OMC during the CMJ showed varied outcomes across peaks and ROM values evaluated (Table 1). The peak positive frontal angle showed the highest reliability with an ICC of 0.517 (95% Confidence Interval (CI)) [-0.040, 0.850]). In contrast, the Peak negative transverse angle registered the lowest reliability, with an ICC of -0.457 (95% CI [-0.940, 0.270]). The ICC values were equally low across other metrics

evaluated. When assessing the LSJ, the agreement between IMU and OMC was generally less. No metric in the LSJ surpassed an ICC value of 0.217, underscoring a low level of concurrence with OMC.

RMSE analysis further highlighted the accuracy of IMU measurements when compared against OMC standards. In the CMJ, the peak positive frontal angle yielded the most minimal deviation with an RMSE of 6.71°. In contrast, the peak positive sagittal angle displayed the most pronounced discrepancy, registering an RMSE of 34.33°. Turning to the LSJ, the ROM frontal angle revealed the least deviation, marked by an RMSE of 11.27°, while the ROM transverse angle was the most divergent with an RMSE of 79.70°.

Moreover, the IMU event detection algorithm successfully detected 98.15% (159 out of 162) of the expected jumps, underscoring its efficacy.

CHAPTER IV: DISCUSSION

The primary goal of this study was to assess the accuracy and reliability of IMU-derived

ankle joint kinematics during CMJ and LSJ and subsequently comparing the peak and ROM

measurements with a conventional OMC system. While our results showed deviations from

prior studies by Gui et al, Seel et al and Song et al[6,13,14] who had success in their computation

and comparison assessments, it's crucial to note the context between investigations. The

simple, ambulatory nature of previous works[6,13,14] is in contrast with the dynamic, acceleration-

based protocols utilized in the current study. This possibly explains the discrepancies in findings.

Interestingly, the current study results align with Fain et al[31], who similarly examined dynamic

movements. Fain et al[31] observed a low level kinematic agreement for the ankle joint during

CMJ with RMSE for peak plantarflexion angle being 46-79% of the OMC and IMU averages.

Specifically, the study's RMSE values were greater than 10° for both peak flexion angle and ROM

despite the utilization of sophisticated computation methods like the Kalman filter sensor fusion

method with magnetometer reference[11]. This highlights the inherent challenges in capturing

accurate ankle kinematics during dynamic tasks using IMUs.

One of the intriguing findings from this study was the moderate ICC and low RMSE for

the peak positive frontal angles. Such outcomes suggest that our methodology holds promise,

particularly in detecting critical ankle movements like inversion during vertical jump landings.

Given that excessive inversion is a predominant cause of ankle sprains [25,33], the potential of this

method in real-world scenarios becomes evident. By leveraging this system, there's a unique

opportunity to elucidate the kinematic patterns underlying ankle sprain injuries. However, it is

imperative to cautiously interpret these results as a whole, considering the low levels of

accuracy and reliability observed in other evaluated peak and ROM measurements. One plausible explanation for these discrepancies lies in the inherent differences in reference determination between IMU and OMC. While the IMU algorithm determines the reference angle from a detected foot-flat segment post-landing for each jump, the OMC system relies on a static model assessed at the beginning of data collection. The dynamic nature of the jumps, coupled with the challenges in accurately detecting the foot-flat segment—defined in our study as a period of minimal acceleration during landing—could significantly influence the derived ankle angles. Additionally, the presence of unavoidable accelerometer noise might have impacted the accuracy of inclination angles used in the complementary filter sensor fusion. As these angles play a limited role in counteracting drifts in the generated angles, their utility in dynamic movements becomes questionable. This affirms the algorithms are more suited for slower movements.

Another noteworthy consideration is the effect of soft tissue artifacts intrinsic to IMU measurements during dynamic motions. These artifacts, emerging from the sensors' non-rigid attachment, can introduce noise which may distort the representation of the actual skeletal movement. This distortion becomes particularly pronounced during rapid movements, where the interplay of muscles and soft tissues is more complex. Fain et al[31] opined that a source of these artifacts could also be from substantial proximal musculature of the limb during these movements. These artifacts, resulting from the non-rigid attachment of the sensors, could introduce noise and distort the actual skeletal movement.

Given these results, it is apparent that this methodology, in comparison with OMC output, falls short in accurately processing dynamic activities. The notable exception is the

measurement of inversion angles during jumps, which exhibits some potential. Potential future

applications and improvements, particularly in dynamic, ballistic movements like CMJ and LSJ,

will involve some strategies. First, establishing a standardized, reference initiation position for

each activity could be a crucial step. This approach would ensure better alignment and

comparability with the OMC's static model, potentially enhancing the accuracy and reliability of

the IMU measurements. Additionally, a comprehensive overhaul of the algorithm is essential to

adequately handle the complexities inherent in such dynamic movements. This refinement

should focus on key aspects like the IMU's propensity to pick up noise, especially during rapid

and high-intensity movements and a more nuanced understanding and integration of the effects

of soft tissue dynamics. Addressing these challenges in the algorithm's design will help in

capturing a more accurate representation of the joint kinematics, particularly in multi-planar

and three-dimensional contexts.

REFERENCES

1. Brockett CL, Chapman GJ. Biomechanics of the ankle. *Orthop Trauma*. 2016;30(3):232-238. doi:10.1016/j.mporth.2016.04.015

2. Cheng P, Oelmann B. Joint-Angle Measurement Using Accelerometers and Gyroscopes—A Survey. *IEEE Trans Instrum Meas*. 2010;59:404-414.

3. Cho YS, Jang SH, Cho JS, et al. Evaluation of Validity and Reliability of Inertial Measurement Unit-Based Gait Analysis Systems. *Ann Rehabil Med*. 2018;42(6):872-883. doi:10.5535/arm.2018.42.6.872

4. Al-Amri M, Nicholas K, Button K, Sparkes V, Sheeran L, Davies JL. Inertial Measurement Units for Clinical Movement Analysis: Reliability and Concurrent Validity. *Sensors*. 2018;18(3):719. doi:10.3390/s18030719

5. Teufl W, Miezal M, Taetz B, Fröhlich M, Bleser G. Validity, Test-Retest Reliability and Long-Term Stability of Magnetometer Free Inertial Sensor Based 3D Joint Kinematics. *Sensors*. 2018;18(7):1980. doi:10.3390/s18071980

6. Gui P, Tang L, Mukhopadhyay S. MEMS based IMU for tilting measurement: Comparison of complementary and Kalman filter based data fusion. *2015 IEEE 10th Conf Ind Electron Appl ICIEA*. Published online 2015:2004-2009.

7. Rico-Garcia M, Botero-Valencia J, Hernández-García R. Vertical Jump Data from Inertial and Optical Motion Tracking Systems. *Data*. 2022;7(8):116. doi:10.3390/data7080116

8. Chen H, Schall MC, Martin SM, Fethke NB. Drift-Free Joint Angle Calculation Using Inertial Measurement Units without Magnetometers: An Exploration of Sensor Fusion Methods for the Elbow and Wrist. *Sensors*. 2023;23(16):7053. doi:10.3390/s23167053

9. Fang Z, Woodford S, Senanayake D, Ackland D. Conversion of Upper-Limb Inertial Measurement Unit Data to Joint Angles: A Systematic Review. *Sensors*. 2023;23(14):6535. doi:10.3390/s23146535

10. Hamdi M, Awad MI, Abdelhameed MM, Tolbah FA. Lower limb motion tracking using IMU sensor network. *2014 Cairo Int Eng Conf CIBEC Giza*. Published online 2014:28-33.

11. Hindle BR, Keogh JWL, Lorimer AV. Validation of Spatiotemporal and Kinematic Measures in Functional Exercises Using a Minimal Modeling Inertial Sensor Methodology. *Sensors*. 2020;20(16):4586. doi:10.3390/s20164586

12. Lee JK, Jeon TH. IMU-Based but Magnetometer-Free Joint Angle Estimation of Constrained Links. *2018 IEEE Sens New Delhi India*. Published online 2018:1-4.

13. Seel T, Raisch J, Schauer T. IMU-Based Joint Angle Measurement for Gait Analysis. *Sensors*. 2014;14(4):6891-6909. doi:10.3390/s140406891

14. Song SY, Pei Y, Hsaio-Wecksler ET. Estimating Relative Angles Using Two Inertial Measurement Units Without Magnetometers. *IEEE Sens J*. 2022;22(20):19688-19699.

15. Zrenner M, Gradl S, Jensen U, Ullrich M, Eskofier BM. Comparison of Different Algorithms for Calculating Velocity and Stride Length in Running Using Inertial Measurement Units. *Sensors*. 2018;18(12):4194. doi:10.3390/s18124194

16. Favre J, Jolles BM, Aissaoui R, Aminian K. Ambulatory measurement of 3D knee joint angle. *J Biomech*. 2008;41(5):1029-1035. doi:10.1016/j.jbiomech.2007.12.003

17. Honert EC, Harrison K, Feeney D. Evaluating footwear "in the wild": Examining wrap and lace trail shoe closures during trail running. *Front Sports Act Living*. 2023;4. Accessed September 22, 2023. https://www.frontiersin.org/articles/10.3389/fspor.2022.1076609

18. Lehmann D, Laidig D, Deimel R, Seel T. Magnetometer-free inertial motion tracking of arbitrary joints with range of motion constraints. *IFAC-Pap*. 2020;53(2):16016-16022. doi:10.1016/j.ifacol.2020.12.401

19. Seel T, Graurock D, Schauer T. Realtime assessment of foot orientation by Accelerometers and Gyroscopes. *Curr Dir Biomed Eng*. 2015;1(1):446-469. doi:10.1515/cdbme-2015-0112

20. Takeda R, Tadano S, Natorigawa A, Todoh M, Yoshinari S. Gait posture estimation using wearable acceleration and gyro sensors. *J Biomech*. 2009;42(15):2486-2494. doi:10.1016/j.jbiomech.2009.07.016

21. Panoutsakopoulos V, Bassa E. Countermovement Jump Performance Is Related to Ankle Flexibility and Knee Extensors Torque in Female Adolescent Volleyball Athletes. *J Funct Morphol Kinesiol*. 2023;8(2):76. doi:10.3390/jfmk8020076

22. Pryhoda M, Wathen R, Dicharry J, et al. Alternative upper configurations during agility-based movements: part 1, biomechanical performance. *Footwear Sci*. 2021;13:1-14. doi:10.1080/19424280.2020.1853824

23. Schmidt M, Jaitner T, Nolte K, Rheinländer C, Wille S, Wehn N. A Wearable Inertial Sensor Unit for Jump Diagnosis in Multiple Athletes. *Proc 2nd Int Congr Sports Sci Res Technol Support*. Published online 2014. Accessed September 22, 2023. https://www.academia.edu/24103953/A_Wearable_Inertial_Sensor_Unit_for_Jump_Diagnosis_in_Multiple_Athletes

24. Panoutsakopoulos V, Kotzamanidou MC, Giannakos AK, Kollias IA. Relationship of Vertical Jump Performance and Ankle Joint Range of Motion: Effect of Knee Joint Angle and Handedness in Young Adult Handball Players. *Sports*. 2022;10(6):86. doi:10.3390/sports10060086

25. Terada M, Gribble PA. Jump Landing Biomechanics During a Laboratory Recorded Recurrent Ankle Sprain. *Foot Ankle Int*. 2015;36(7):842-848. doi:10.1177/1071100715576517

26. Work with Vicon IMUs - Nexus 2.12 Documentation - Vicon Documentation. Accessed October 27, 2023. https://docs.vicon.com/display/Nexus212/Work+with+Vicon+IMUs

27. Jaitner T, Schmidt M, Nolte K, Rheinländer C, Wille S, Wehn N. Vertical jump diagnosis for multiple athletes using a wearable inertial sensor unit. *Sports Technol*. 2015;8(1-2):51-57. doi:10.1080/19346182.2015.1117476

28. Smith P, Bedford A. A FLEXIBLE METHOD OF JUMP AND HIGH INTENSITY EVENT DETECTION. Published online July 1, 2018.

29. Wu G, Siegler S, Allard P, et al. ISB recommendation on definitions of joint coordinate system of various joints for the reporting of human joint motion—part I: ankle, hip, and spine. *J Biomech*. 2002;35(4):543-548. doi:10.1016/S0021-9290(01)00222-6

30. Chai T, Draxler RR. Root mean square error (RMSE) or mean absolute error (MAE)? – Arguments against avoiding RMSE in the literature. *Geosci Model Dev*. 2014;7(3):1247-1250. doi:10.5194/gmd-7-1247-2014

31. Fain A, Hindle B, Andersen J, et al. TRANSFERABILITY OF A PREVIOUSLY VALIDATED IMU SYSTEM FOR LOWER EXTREMITY KINEMATICS. *ISBS Proc Arch*. 2022;40(1):183.

32. Shrout PE, Fleiss JL. Intraclass correlations: uses in assessing rater reliability. *Psychol Bull*. 1979;86(2):420-428. doi:10.1037//0033-2909.86.2.420

33. Wu HW, Liang KH, Lin YH, Chen YH, Hsu HC. Biomechanics of ankle joint during landing in counter movement jump and straddle jump. In: *2009 IEEE 35th Annual Northeast Bioengineering Conference*. ; 2009:1-2. doi:10.1109/NEBC.2009.4967733

Jan 20, 2023 1:48:49 PM CST

Michael Torry
Kinesiology & Recreation

Re: Initial - IRB-2022-341 Measurement of Ankle Joint kinematics Using IMUs during Countermovement jump and Skater jump

Dear Dr. Michael Torry:

Thank you for submitting your study for review. The Illinois State University Human Subjects Review Board has rendered the decision below for Measurement of Ankle Joint kinematics Using IMUs during Countermovement jump and Skater jump.

Decision: No Human Subjects Research

It was determined that this study did not meet the Federal Regulation's definition of human subject research under the Revised Common Rule. Therefore, IRB review is not necessary.
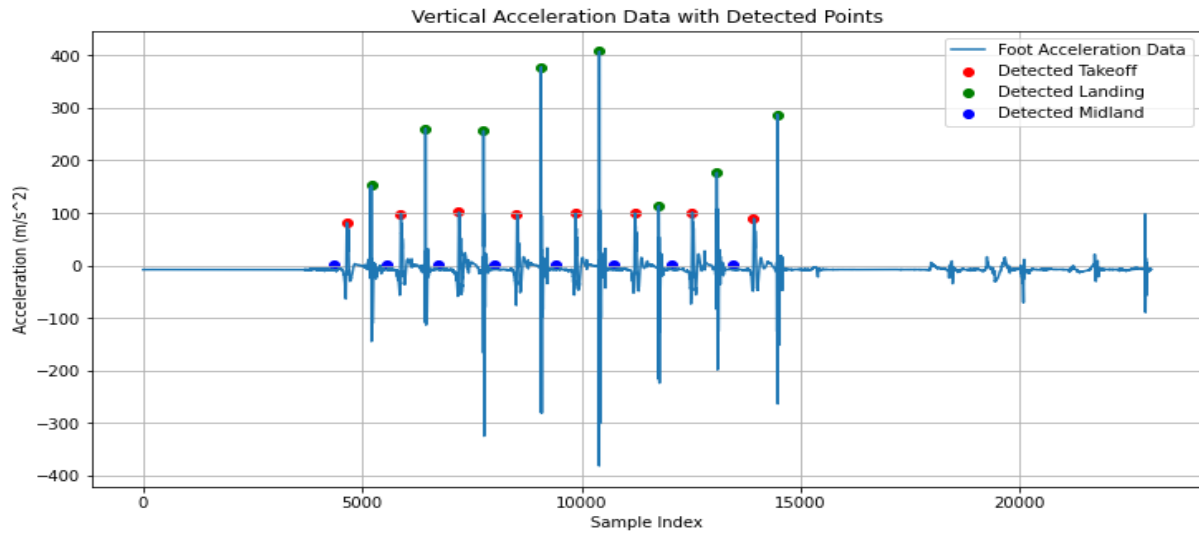
Any modifications that would impact this determination should be submitted for further review.

Sincerely,

The Research Ethics and Compliance Office

Figure A -IRB Consent from Illinois State University allowing use of deidentified data.

Figure B-1 - Plot of vertical acceleration data showing successful events detection to show jump phases.
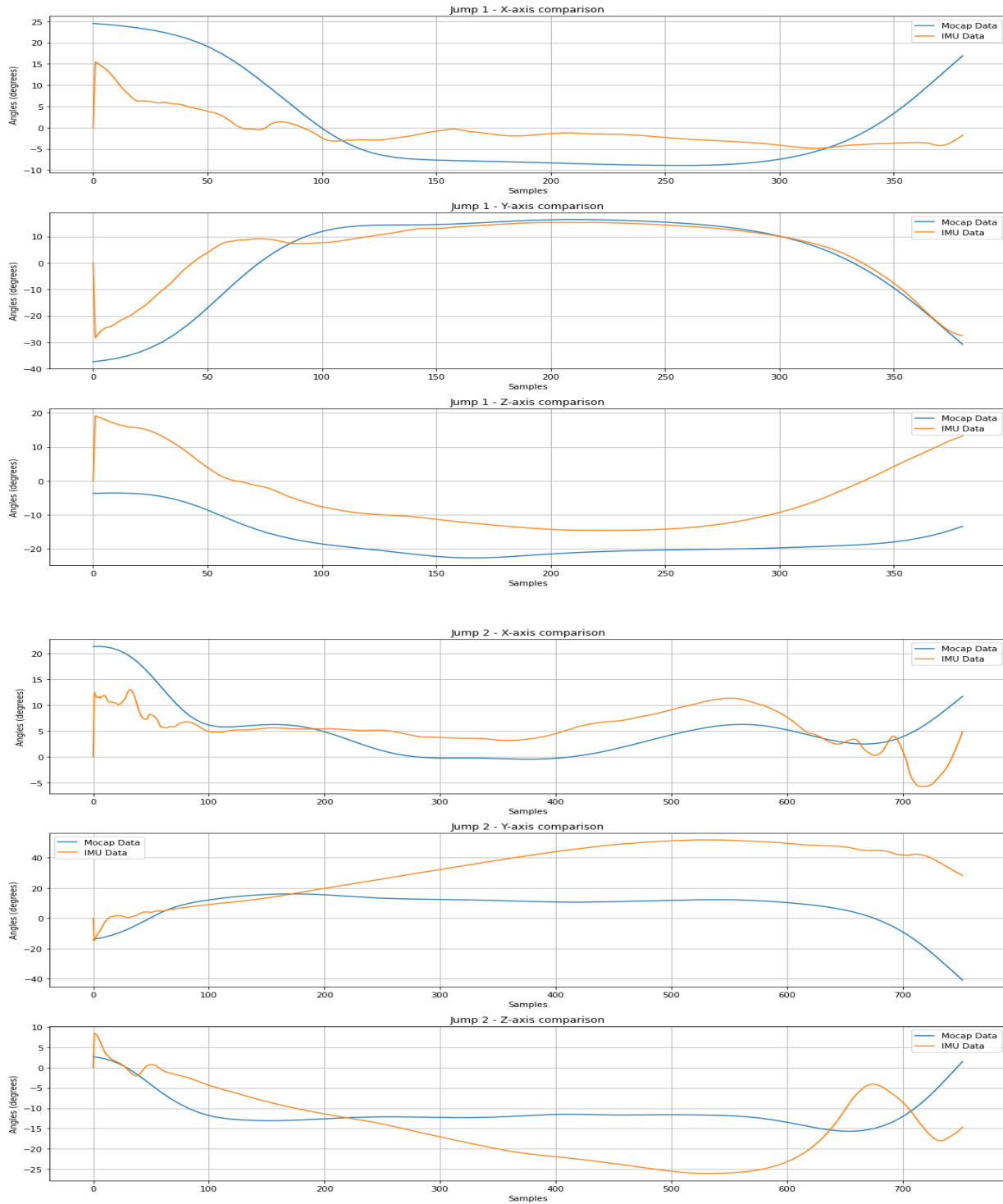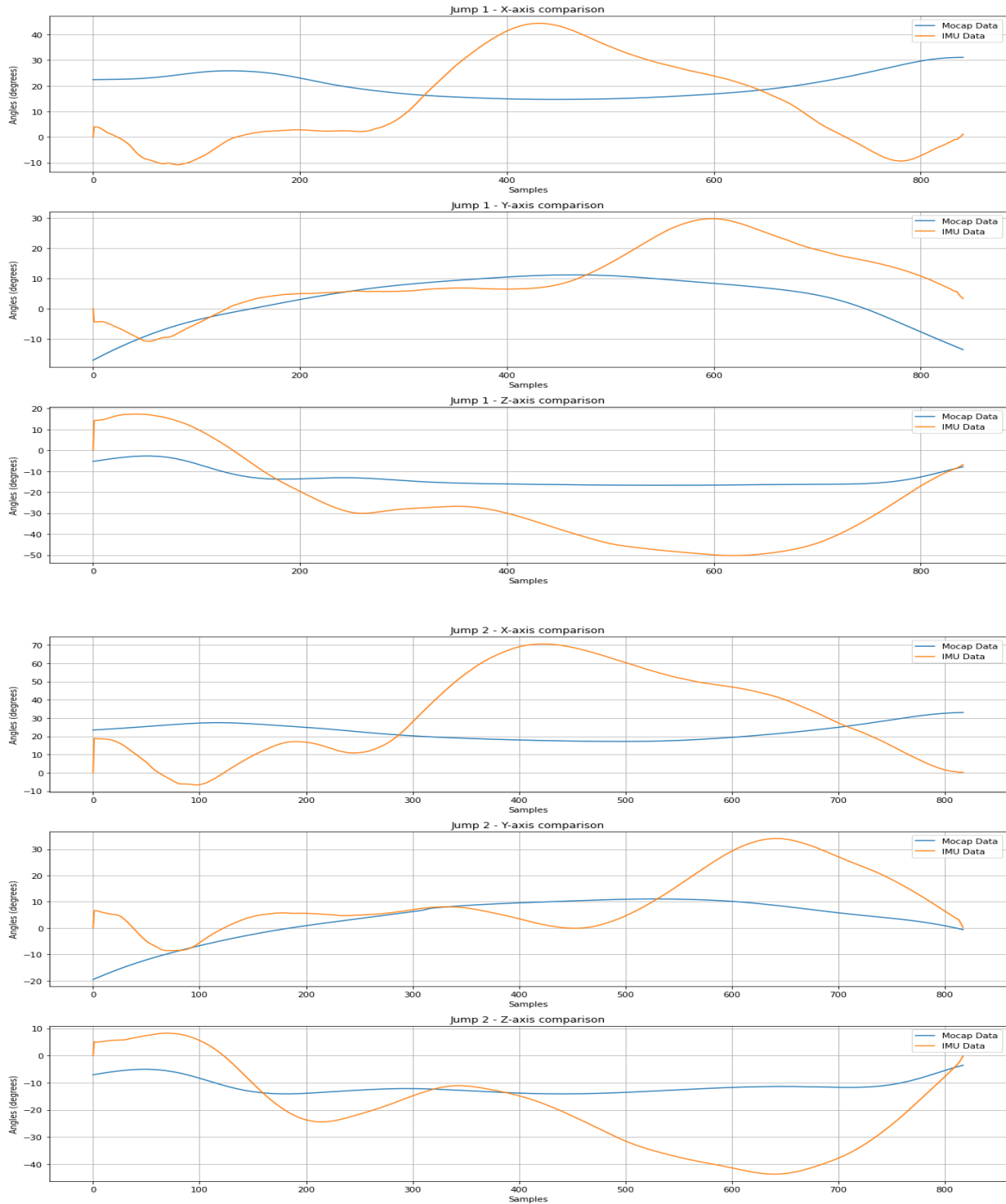
Figure B-2 – Comparative Analysis of IMU and OMC Derived Ankle Joint Angles in CMJ. X-axis represents the ankle inversion/eversion, Y-axis represents plantarflexion/dorsiflexion and Z-axiz represents internal and external rotation.

Figure B-3 - Comparative Analysis of IMU and OMC Derived Ankle Joint Angles in LSJ. X-axis represents the ankle inversion/eversion, Y-axis represents plantarflexion/dorsiflexion and Z-axiz represents internal and external rotation.